Blackbody Emission from Light Interacting with an Effective Moving Dispersive Medium

M. Petev,[1] N. Westerberg,[1] D. Moss,[1] E. Rubino,[2] C. Rimoldi,[2] S. L. Cacciatori,[2] F. Belgiorno,[3] and D. Faccio[1,*]

[1]School of Engineering and Physical Sciences, SUPA, Heriot-Watt University, Edinburgh EH14 4AS, United Kingdom
[2]Dipartimento di Scienza e Alta Tecnologia, Università dell'Insubria, Via Valleggio 11, IT-22100 Como, Italy
[3]Dipartimento di Matematica, Politecnico di Milano, Piazza Leonardo 32, 20133 Milano, Italy

(Received 22 March 2013; published 26 July 2013)

Intense laser pulses excite a nonlinear polarization response that may create an effective flowing medium and, under appropriate conditions, a blocking horizon for light. Here, we analyze in detail the interaction of light with such laser-induced flowing media, fully accounting for the medium dispersion properties. An analytical model based on a first Born approximation is found to be in excellent agreement with numerical simulations based on Maxwell's equations and shows that when a blocking horizon is formed, the stimulated medium scatters light with a blackbody emission spectrum. Based on these results, diamond is proposed as a promising candidate medium for future studies of Hawking emission from artificial, dispersive horizons.

DOI: 10.1103/PhysRevLett.111.043902 PACS numbers: 42.65.Hw, 04.60.−m, 42.50.−p

Recent developments in the understanding of light propagation have led to evidence that by using intense laser pulses propagating in a nonlinear medium, it is possible to create an effective medium that flows with the same speed as the laser pulse, i.e., at speeds close to or, as a consequence of dispersion, even higher than the speed of light at other frequencies in the medium [1–9]. Indeed, in a medium with a third order (also called "Kerr") nonlinear polarization response, the refractive index of the medium is given by $n = n_0 + n_2 I(z - vt)$, where n_0 is the background index, n_2 is the nonlinear Kerr index, and $I(z - vt)$ is the laser-pulse intensity profile, traveling along the z direction with velocity v. In a typical condensed medium, e.g., glass, the maximum amplitude of the laser-pulse-induced refractive index perturbation is $\delta n_{\max} = n_2 I_{\max} \sim 0.01$–$0.001$. This is sufficient to scatter light, e.g., either light from the laser pulse itself (the self-scattering process) or from a second weak probe pulse (the induced scattering process).

Under appropriate conditions, one may also potentially observe induced scattering (and excitation) of photons that originate from the vacuum state. One motivation for studying such an effect lies in the prediction that the δn may be described in terms of a horizon that mimics the event horizon of a gravitational black hole [1–7]. Indeed, in the absence of material dispersion, it is possible to write the effective spacetime metric for the moving δn as $ds^2 = c^2 dt^2 + (dr - V dt)^2$. This is equivalent to the Painlevé-Gullstrand metric showing that in the reference frame of the δn, the medium is effectively flowing with speed V, which is a Galilean velocity $(-\infty < V < +\infty)$ and is determined by n and v. A horizon is formed when $V = c$ [5,10]. Interaction with the vacuum state leads to the emission of photon pairs that are analogous to Hawking emission from a black hole. Recent measurements claimed the observation of a spontaneous emission from a laser-pulse-induced moving δn that appeared to have some of the features predicted for the analog Hawking emission [11,12]. However, these measurements are not considered as conclusive and further evidence is required [13–15].

In this Letter, we investigate in detail the interaction between a δn moving at a generic speed v and a probe light pulse. Our analytical and numerical models fully account, without any approximations for material dispersion, for the full shape of the δn and allow a comprehensive analysis of the interaction dynamics for varying δn speed. The input probe pulse is scattered into two output modes, one with positive and the other with negative comoving frequencies [16]. A remarkable feature of this stimulated emission is that the negative mode emissivity is dictated by a blackbody law with a temperature that is directly related to the steepness of the moving δn. This prediction is also fully confirmed analytically within a Born approximation model that provides physical insight into the scattering mechanism. The blackbody emission is predicted to occur for δn speeds such that the light pulse is slowed to the point that it cannot traverse the δn—the δn has a blocking horizon. It is in this regime that we propose a setting for future experiments in diamond that exhibits the required conditions to observe analog Hawking emission.

Scattering from a moving δn.—A soliton propagating in a dispersive medium will shed light through a mechanism known as resonant (or dispersive wave) radiation (RR) [17–20]. This emission may be described as a self-induced scattering process whereby light from the soliton is scattered into a frequency-shifted mode by the self-induced Kerr δn. It was recently shown that a second scattered mode also exists: this mode has negative frequency in the reference frame comoving with the soliton and has been called "negative-frequency resonant radiation" (NRR) [16]. Both of these modes are found within the framework

of a model that neglects all nonlinear effects and simply considers the soliton δn and models how light is scattered within the first Born approximation [21]. The model therefore generalizes RR and NRR generation beyond soliton physics to also include systems that do not support solitons (e.g., a three-dimensional pulse with transverse spatial dynamics or an intense pulse in the normal group velocity dispersion regime). The scattered amplitudes of the two modes are given by [21]

$$S(\omega_{\mathrm{RR}}) = i\frac{v\omega_{\mathrm{RR}}^2 n_0}{2c^2 k_z(\omega_{\mathrm{RR}})} e^{i[(\omega_{\mathrm{RR}}-\omega_{\mathrm{IN}})z/v]}\hat{R}(\omega_{\mathrm{RR}}-\omega_{\mathrm{IN}}), \quad (1)$$

$$S(\omega_{\mathrm{NRR}}) = i\frac{v\omega_{\mathrm{NRR}}^2 n_0}{2c^2 k_z(\omega_{\mathrm{NRR}})} e^{i[(\omega_{\mathrm{NRR}}+\omega_{\mathrm{IN}})z/v]}\hat{R}(\omega_{\mathrm{NRR}}+\omega_{\mathrm{IN}}), \quad (2)$$

where $\hat{R}$ is the δn Fourier transform and $\omega_{\mathrm{RR,NRR,IN}}$ are the RR, NRR, and input probe pulse frequencies.

In the following, we present a series of numerical simulations and a comparison with predictions based on the Born approximation equations (1) and (2) with which we estimate the amplitudes of the RR and NRR waves generated by an input probe pulse interacting with a moving δn, for varying frequency of the input pulse. The system considered is depicted in Fig. 1—a probe light pulse interacts with the trailing edge of a moving δn. The δn may thus be modeled using any function that describes a rising refractive index front (two examples are shown in the figure). Backward propagating modes are neglected on the basis that their overlap times with the input pulse and δn are extremely short and they will therefore carry negligible energy. The numerical simulations were carried out using both a finite difference time domain (FDTD) [22] and the unidirectionnal pulse propagation equation (UPPE) [21,23] algorithms all under the same input conditions. Both methods directly solve Maxwell's equations; however, the FDTD algorithm supports backward propagating modes while the UPPE does not. There were no discernible differences between the outputs of these two codes, hence lending further support to neglecting the backward modes. In Fig. 2, we show examples obtained with the FDTD code

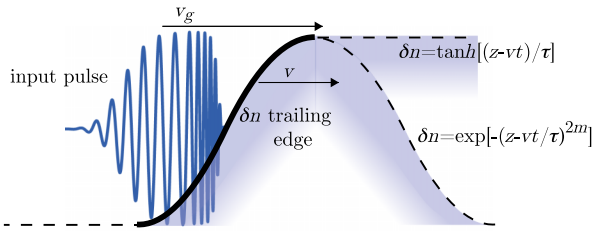

FIG. 1 (color online). Schematic drawing of interaction geometry: the input light pulse propagates with speed v_g, catches up and interacts with the trailing edge (thick solid curve) of the moving δn, propagating with speed $v \lesssim v_g$.

with $\delta n = \delta n_{\mathrm{max}} \exp\{-[(z-vt)^2/\sigma^2]^m\}$, where $\delta n_{\mathrm{max}} = 0.01$; σ and m are chosen so that the δn front has a 7 fs rise time and also such that this rise time is much shorter than the overall width of the δn, thus ensuring that light only interacts with the trailing edge. The dispersion is chosen so as to resemble that of diamond and is shown in the figure in (ω', ω) frequency coordinates, where primed quantities indicate that they refer to the comoving reference frame $\omega' = (\omega - vk)$, where k is the light pulse wave vector.

Figure 2(a) shows the temporal envelope profile of an input 5 μm wavelength probe beam interacting with the δn in the comoving frame for the generic case in which the δn speed $v = 1.9 \times 10^8$ m/s is too slow to actually completely block the impinging light for $\delta n_{\mathrm{max}} = 0.01$. We refer to this as the "nonblocking" case: the input light will be transmitted through the δn into a mode indicated with F and will only be partly scattered into the RR and NRR modes that are reflected backward in the comoving frame (but are traveling forward in the laboratory frame). This partial conversion is also clear in the frequency spectrum evolution in Fig. 2(b) that shows generated peaks that are in excellent agreement with the frequencies predicted from momentum conservation, i.e., comoving frequency ω'

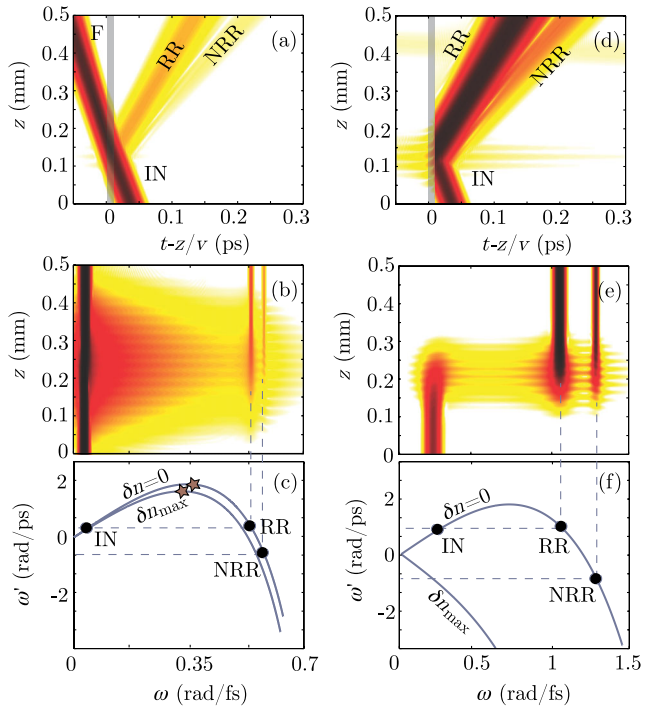

FIG. 2 (color online). Example of a numerically simulated interaction of a probe pulse with a moving δn. (a),(b) and (c) show the temporal envelope profile evolution, spectral evolution and relevant dispersion curves, respectively, for the case in which the δn moves too slowly to form a blocking horizon. (d),(e) and (f) show similar figures for a faster δn such that a blocking horizon is formed. The δn rising front is shown as a grey shaded area in (a) and (d). All intensity plots are shown over 4 decades in logarithmic scale.

conservation shown as the horizontal dashed lines intersecting the dispersion relation in Fig. 2(c). Generalized Manley-Rowe (photon number balance) relations may be derived for an effective moving medium that, accounting for the modes present in this case, reads as $|F|^2 + |\mathrm{RR}|^2 - |\mathrm{NRR}|^2 = 1$, where $|\cdot|$ indicates the mode photon number normalized with respect to the input mode [24,25].

Figures 2(c)–2(e) show similar results, but now $v = 2.07 \times 10^8$ m/s has been increased such that the input light pulse is slowed down upon interacting with the δn rising front to the point that its group velocity becomes equal to v; i.e., the δn presents a "blocking horizon" for light. In this case, the input mode is completely converted to the RR and NRR modes, and $|\mathrm{RR}|^2 - |\mathrm{NRR}|^2 = 1$.

We now examine the ratio $r = |\mathrm{NRR}|^2/|\mathrm{RR}|^2$ for varying input frequency. In Fig. 3(a), we show a typical example for the blocking case in logarithmic scale (the red points are results from numerical simulations, and the solid line is a linear fit). Similar results are found for all values of v, i.e., also in the nonblocking case. The surprising feature here is that r has a clear exponential dependence over more than eight decades. If we then combine this exponential dependence $r = \exp(-\alpha\omega')$ with the generalized Manley-Rowe relations, we find that

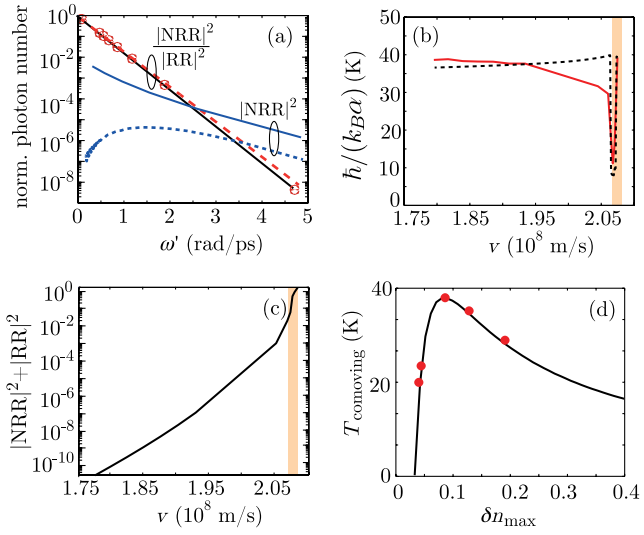

FIG. 3 (color online). (a) Numerical simulation for $v = 1.9 \times 10^8$ m/s of $r = |\mathrm{NRR}|^2/|\mathrm{RR}|^2$ for varying input frequency (dots) and best fit with exponential function (solid line). Dashed line—Born approximation calculation. Also shown is the normalized photon number $|\mathrm{NRR}|^2$ for the blocking (solid blue line) and nonblocking (dotted line) cases. (b) $\hbar/k_B\alpha$ [derived from graphs as in (a)] for varying δn speed—simulations (solid line) and Born approximation model (dashed line). The shaded area indicates speeds for which a blocking horizon is formed. (c) Total normalized photon count for varying speed. (d) Comparison between numerically estimated emission temperature $T = \hbar/k_B\alpha$ (dots) and theoretical Hawking emission temperature estimated from the δn gradient (solid line) for varying maximum index change $\delta n_{\max}$ (blocking case).

$|\mathrm{NRR}|^2 = (1 - |F|^2)/[\exp(\alpha\omega') - 1]$. In the blocking case ($|F|^2 = 0$), this implies that the NRR mode emission follows a blackbody law with temperature given by $T = \hbar/(k_B\alpha)$. The NRR photon number will thus diverge close to $\omega' = 0$, as shown in Fig. 3(a) (solid line indicated with "NRR"). The moving δn is therefore effectively transforming the input light, regardless of its state, into an output NRR mode that has a comoving blackbody spectrum. We can also evaluate r directly from the first Born approximation relations [Eqs. (1) and (2)], and the same exponential dependence for r is found [shown as a dashed line in Fig. 3(a)]. For a wide range of steplike functions, the Born approximation can even be solved exactly and thus proves the robustness of this result (see the Supplemental Material [26]).

In Fig. 3(b), we show the $\hbar/k_B\alpha$ obtained from similar curves as shown in Fig. 3(a) for varying δn speeds: the solid line is the result from numerical simulations, the dashed line shows the Born approximation result, and the two curves are in overall good agreement. However, we note that in crossing over into the nonblocking case, the appearance of the additional transmitted mode ($|F|^2 > 0$) significantly distorts the blackbody spectrum. Indeed, if we plot the NRR photon number for a nonblocking case [dotted line in Fig. 3(a)], we see that at small frequencies the mode number drops to zero rather than diverging, as would be expected for a 1D blackbody emission. This is in keeping with quantum calculations in a generic "flowing fluid" setting [27] and can be understood by noting that for high enough frequencies, a blocking horizon is still present [region between the dispersion curve maxima indicated with stars in Fig. 2(c)] but low frequencies are not blocked at all, implying that the interaction time with the δn trailing edge is significantly reduced and any scattering process is suppressed. This suppression is also observed in Fig. 3(c), which shows the total photon number $|\mathrm{NRR}|^2 + |\mathrm{RR}|^2$ evaluated from the numerical simulations. As can be seen, this number varies by several orders of magnitude with varying v and is dramatically enhanced only in the presence of a blocking horizon.

We note that a blocking horizon may be likened to a white hole horizon, which in turn has been predicted to lead to Hawking emission [1,4,5,7,28], i.e., emission of a blackbody spectrum. In the presence of a blocking horizon, we may therefore evaluate the Hawking temperature according to $T = (1/2\pi)\gamma^2 v|dn/dt|$ (evaluated at the horizon) [5]. In Fig. 3(d), we compare the (comoving) Hawking temperature (solid curve) and the numerically estimated temperatures (red dots) for δn with a fixed v and varying $\delta n_{\max}$. As can be seen, the agreement is excellent over a wide range of values, including for $\delta n_{\max}$ values that are experimentally accessible through the nonlinear Kerr effect.

We note that in the blocking case, the Manley-Rowe relations imply that $|\mathrm{RR}|^2 + |\mathrm{NRR}|^2 > 1$; i.e., the photon

numbers are amplified (at the expense of the moving δn) [21]. Therefore, if the input probe pulse were to be reduced to the level of the quantum noise fluctuations, then the results shown above predict the spontaneous emission of a blackbody spectrum. In other words, the noise of the amplifier is characterized by a temperature that remains constant across all frequencies. This is therefore a somewhat different kind of amplifier with respect to better known examples in optics, e.g., optical parametric amplifiers that have a noise temperature that scales linearly with frequency $T = \hbar\omega/k_B$ [29]. Moreover, the link with gravitational horizons implies that the amplifier noise measured in an actual experiment may be likened to spontaneous Hawking radiation. The blackbody dependence implies that the amplifier gain scales as $1/\omega'$ for $\omega' \to 0$. In the comoving frame, light is coupled between modes that have a constant or nearly constant $\omega' \sim 0$. Looking at Fig. 2(f), we see that if the input mode has a laboratory frequency ω close to zero, then the output mode will appear at high frequencies, typically in the UV region, in the laboratory frame. The amplifier therefore converts radiation from the low to the high (lab frame) frequency modes and the $1/\omega'$ blackbody divergence; i.e., Hawking emission will appear as a divergence (or peak) centered at the UV lab frame frequency.

The high amplification gain when coupling between $\omega' \sim 0$ modes also indicates possible methods for efficiently observing these scattering effects and possible applications. For example, in Fig. 4, we show numerical simulations of a weak 15 THz probe (20 μm wavelength) pulse interacting with a Ti:sapphire laser pulse with 800 nm wavelength, 60 fs duration, and input intensity 80 TW/cm^2, propagating in a 500 μm thick diamond sample. These simulations were performed using two UPPE equations, one for the pump and one for the THz pulse that are coupled only through a nonlinear cross-phase-modulation term in the THz pulse equation $\propto 2n_2 I$ (details of the code can be found, e.g., in Ref. [21]). The self-phase-modulation term $\propto n_2 I$ is included in the 800 nm pump equation, but four wave mixing and third harmonic generation have been purposely neglected. There is no blocking horizon for the probe pulse, but nevertheless the spectrum clearly shows relatively efficient scattering to the UV that occurs predominantly when a shock front, i.e., the steepest gradient, forms on the pump pulse [indicated by an arrow in Fig. 4(a)] in agreement with Eqs. (1) and (2). Most interestingly, the output mode is peaked around the $\omega' \sim 0$, corresponding to a lab frequency of 7 rad/fs (270 nm wavelength). In other words, laboratory reference frame frequencies in the THz or multi-THz region are already sufficiently low to excite the $1/\omega'$ gain of the amplifier. This in turn provides indications of the spectral range of the noise fluctuations that may be spontaneously excited by the δn and lead to a spontaneous (i.e., seeded by thermal or vacuum noise) emission peak in the UV. At room

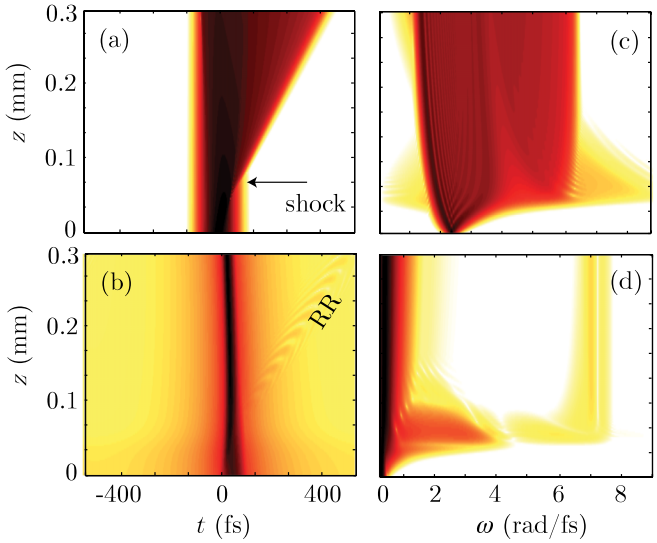

FIG. 4 (color online). Numerical simulation of the nonlinear propagation of an 800 nm pump pulse and a copropagating 15 THz probe pulse (shown in logarithmic scale over four decades). Temporal profile evolution of (a) the 800 nm pump pulse and of (b) the THz pulse. The arrow indicates the propagation distance at which a shock front forms on the pump pulse. "RR" indicates emission from the THz pulse scattered from the pump shock front. (c) Pump pulse spectral evolution. The THz pulse spectrum (six decades in logarithmic scale) in (d) shows a clear peak centered around the $\omega' = 0$ point, corresponding to a 7 rad/fs lab frame frequency.

temperature, the background blackbody photon mode density at 15 THz is $\sim 10^5$ and thus significantly larger than the quantum vacuum noise mode density equal to $1/2$ a photon per mode: spontaneous emission will be seeded by the thermal background. However, it is sufficient to cool the diamond sample to $\sim$30 K to invert the situation such that thermal fluctuations are dominated by more than 1 order of magnitude by quantum vacuum noise.

Conclusions.—A numerical and analytical evaluation based on the Born scattering approximation predicts that light is dramatically transformed by a moving medium. The Born approximation model used here could also be extended to provide exact analytical relations and study scattering phenomena in other systems in which linear waves interact with a moving, dispersive medium, e.g., gravity waves in water or acoustic oscillations in Bose-Einstein condensates. Optical horizons have been proposed for the measurement of Hawking emission but also for all-optical transitors [30]. Other applications of an effective moving medium to be considered in future work could be relatively efficient THz detection by frequency conversion in diamond (even without a horizon, as shown in Fig. 4) or generation of squeezed vacuum states in the UV region.

D. F. acknowledges discussions with I. Carusotto and S. Finazzi and financial support from the Engineering

and Physical Sciences Research Council (EPSRC) Grant No. EP/J00443X/1 and from the European Research Council under the European Union's Seventh Framework Programme (No. FP/2007-2013)/ERC Grant Agreement No. 306559.

*d.faccio@hw.ac.uk

[1] T. G. Philbin, C. Kuklewicz, S. Robertson, S. Hill, F. König, and U. Leonhardt, Science **319**, 1367 (2008).
[2] D. Faccio, Contemp. Phys. **53**, 97 (2012).
[3] D. Faccio, S. Cacciatori, V. Gorini, V. G. Sala, A. Averchi, A. Lotti, M. Kolesik, and J. V. Moloney, Europhys. Lett. **89**, 34 004 (2010).
[4] S. Finazzi and I. Carusotto, Phys. Rev. A **87**, 023803 (2013).
[5] F. Belgiorno, S. L. Cacciatori, G. Ortenzi, L. Rizzi, V. Gorini, and D. Faccio, Phys. Rev. D **83**, 024015 (2011).
[6] S. L. Cacciatori, F. Belgiorno, V. Gorini, G. Ortenzi, L. Rizzi, V. G. Sala, and D. Faccio, New J. Phys. **12**, 095021 (2010).
[7] C. Barceló, S. Liberati, and M. Visser, Living Rev. Relativity **14**, 3 (2011).
[8] A. Guerreiro, A. Ferreira, and J. T. Mendonça, Phys. Rev. A **83**, 052302 (2011).
[9] F. Belgiorno, S. L. Cacciatori, G. Ortenzi, V. G. Sala, and D. Faccio, Phys. Rev. Lett. **104**, 140403 (2010).
[10] A. J. S. Hamilton and J. P. Lisle, Am. J. Phys. **76**, 519 (2008).
[11] F. Belgiorno, S. L. Cacciatori, M. Clerici, V. Gorini, G. Ortenzi, L. Rizzi, E. Rubino, V. G. Sala, and D. Faccio, Phys. Rev. Lett. **105**, 203901 (2010).
[12] E. Rubino, F. Belgiorno, S. L. Cacciatori, M. Clerici, V. Gorini, G. Ortenzi, L. Rizzi, V. G. Sala, M. Kolesik, and D. Faccio, New J. Phys. **13**, 085005 (2011).
[13] R. Schützhold and W. G. Unruh, Phys. Rev. Lett. **107**, 149401 (2011).
[14] S. Liberati, A. Prain, and M. Visser, Phys. Rev. D **85**, 084014 (2012).
[15] W. G. Unruh and R. Schützhold, Phys. Rev. D **86**, 064006 (2012).
[16] E. Rubino, J. McLenaghan, S. C. Kehr, F. Belgiorno, D. Townsend, S. Rohr, C. E. Kuklewicz, U. Leonhardt, F. Konig, and D. Faccio, Phys. Rev. Lett. **108**, 253901 (2012).
[17] P. K. A. Wai, C. R. Menyuk, Y. C. Lee, and H. H. Chen, Opt. Lett. **11**, 464 (1986).
[18] N. Akhmediev and M. Karlsson, Phys. Rev. A **51**, 2602 (1995).
[19] D. V. Skryabin and A. V. Yulin, Phys. Rev. E **72**, 016619 (2005).
[20] J. M. Dudley, G. Genty, and S. Coen, Rev. Mod. Phys. **78**, 1135 (2006).
[21] E. Rubino, A. Lotti, F. Belgiorno, S. L. Cacciatori, A. Couairon, U. Leonhardt, and D. Faccio, Sci. Rep. **2**, 932 (2012).
[22] A. Taflove and S. C. Hagness, *Computational Electrodynamics: The Finite-Difference Time-Domain Method* (Artech House, London, 2005).
[23] M. Kolesik and J. V. Moloney, Phys. Rev. E **70**, 036604 (2004).
[24] L. A. Ostrovskii, Sov. Phys. JETP **34**, 293 (1972).
[25] Y. A. Kravtsov, L. A. Ostrovskii, and N. S. Stepanov, Proc. IEEE **62**, 1492 (1974).
[26] See Supplemental Material at http://link.aps.org/supplemental/10.1103/PhysRevLett.111.043902 for a study of the case of a superluminal refractive medium, details of how the photon numbers are calculated and some simplified δn profiles for which the Born approximation model is solved analytically.
[27] S. J. Robertson, J. Phys. B **45**, 163001 (2012).
[28] W. G. Unruh, Phys. Rev. Lett. **46**, 1351 (1981).
[29] W. H. Louisell, A. Yariv, and A. E. Siegman, Phys. Rev. A **124**, 1646 (1961).
[30] A. Demircan, Sh. Amiranashvili, and G. Steinmeyer, Phys. Rev. Lett. **106**, 163901 (2011).